Supplementary Material for "Estimating Individualized Treatment Rules for Multicategory Type 2 Diabetes Treatments Using Electronic Health Records"

Jitong Lou, Yuanjia Wang, Lang Li and Donglin Zeng

S.1 Simulation Study of M-learning

In this section, we perform a simulation study to investigate the finite sample performance of the proposed M-learning and compare with the M-learning without latent subgroup information (Wu et al., 2020). Since we are not allowed the release the EHR dataset, we use this simulation study as an example and publish an R package `MultiMlearn` on `https://github.com/jitonglou/MultiMlearn` to implement the proposed approach. Besides this document, a vignette of our package is also available on `https://github.com/jitonglou/MultiMlearn/tree/master/doc`.

S.1.1 General Setting

Suppose there are N subjects, K treatments, and J subject groups. Denoting $\boldsymbol{x}_i$ to the p-dimensional covariates and $A_i \in \{1, \ldots, K\}$ to the treatment of subject i, we generate R_{ij}, the continuous outcome for subject $i \in \{1, \ldots, N\}$ who belongs to group $j \in \{1, \ldots, J\}$, from

$$R_i = \mu(\boldsymbol{x}_i) + \delta_j(\boldsymbol{x}_i) + \epsilon_i, \tag{1}$$

where $\delta_j(x_i) = \sum_{k=1}^{K} f_{jk}(\boldsymbol{x}_i) I(A_i = k)$. Each covariate is generated by the uniform distribution from -1 to 1, and ϵ_i follows the standard normal distribution. The true propensity score is specified as

$$P(A = k|\boldsymbol{x}) \equiv \pi(A = k, \boldsymbol{x}) = \frac{\exp\{X_k + X_{k+1}\}}{\sum_{m=1}^{K} \exp\{X_m + X_{m+1}\}}. \tag{2}$$

The performance of $D(\boldsymbol{x})$, an ITR, is evaluated by the empirical value function

$$\frac{\sum_{i=1}^{N} \mathbb{I}\left(A_i = D(\boldsymbol{x}_i)\right) R_i / \pi\left(A_i, \boldsymbol{x}_i\right)}{\sum_{i=1}^{N} \mathbb{I}\left(A_i = D(\boldsymbol{x}_i)\right) / \pi\left(A_i, \boldsymbol{x}_i\right)}, \tag{3}$$

and the misclassification rate

$$1 - \frac{1}{N} \sum_{i=1}^{N} \mathbb{I}\left(D(\boldsymbol{x}_i) = \arg\max_{A} R_i\right). \tag{4}$$

A higher empirical value and a lower misclassification rate are more desirable.

S.1.2 Simulation Scenario

The covariate vector $\boldsymbol{x}_i$ was set to be $p = 20$ dimensional. Moreover, we set the number of treatments $K = 4$, and the number of groups $J = 4$. The main effect function

$$\mu(\boldsymbol{x}) = 1 + X_1 + X_2. \tag{5}$$

Additionally, we let the interaction function $\delta_j(\boldsymbol{x})$ include polynomial interaction effects. Specifically,

$$\begin{aligned}
\delta_1(\boldsymbol{x}) &= (0.2 + X_1^2 + X_2^2 + X_3^2 + X_4^2)\mathbb{I}(A_i = 1) + (0.2 + X_1^2 - X_2^2 + X_3^2 - X_4^2)\mathbb{I}(A_i = 2) \\
&+ (0.2 + X_1^2 - X_2^2 - X_3^2 + X_4^2)\mathbb{I}(A_i = 3) + (0.2 - X_1^2 - X_2^2 + X_3^2 - X_4^2)\mathbb{I}(A_i = 4), \\
\delta_2(\boldsymbol{x}) &= (0.2 + X_1^2 + X_2^2 + X_3^2 + X_4^2)\mathbb{I}(A_i = 2) + (0.2 + X_1^2 - X_2^2 + X_3^2 - X_4^2)\mathbb{I}(A_i = 3) \\
&+ (0.2 + X_1^2 - X_2^2 - X_3^2 + X_4^2)\mathbb{I}(A_i = 4) + (0.2 - X_1^2 - X_2^2 + X_3^2 - X_4^2)\mathbb{I}(A_i = 1), \\
\delta_3(\boldsymbol{x}) &= (0.2 + X_1^2 + X_2^2 + X_3^2 + X_4^2)\mathbb{I}(A_i = 3) + (0.2 + X_1^2 - X_2^2 + X_3^2 - X_4^2)\mathbb{I}(A_i = 4) \\
&+ (0.2 + X_1^2 - X_2^2 - X_3^2 + X_4^2)\mathbb{I}(A_i = 1) + (0.2 - X_1^2 - X_2^2 + X_3^2 - X_4^2)\mathbb{I}(A_i = 2), \\
\delta_4(x) &= (0.2 + X_1^2 + X_2^2 + X_3^2 + X_4^2)\mathbb{I}(A_i = 4) + (0.2 + X_1^2 - X_2^2 + X_3^2 - X_4^2)\mathbb{I}(A_i = 1) \\
&+ (0.2 + X_1^2 - X_2^2 - X_3^2 + X_4^2)\mathbb{I}(A_i = 2) + (0.2 - X_1^2 - X_2^2 + X_3^2 - X_4^2)\mathbb{I}(A_i = 3).
\end{aligned} \tag{6}$$

Therefore, the optimal treatments for group 1, 2, 3, and 4 are treatment 1, 2, 3, and 4, respectively.

We examined the proposed method for sample size $N = 200, 400,$ and 800. Each simulation was repeated for 100 times. We employed random forests to estimate the propensity and prognostic scores. Using the `caret` package (Kuhn, 2008) in R, we selected the tuning parameters by 10-fold cross-validation with 3 repeats. In weighted support vector machines (SVMs), we used the radial basis function (RBF) kernel to optimize the objective function. We selected the cost parameter from $\left\{2^k : k = 0, \pm 1, \ldots, \pm 15\right\}$ using 5-fold cross-validation, and we calculated the bandwidth parameter of each RBF kernel according to a data-driven method which could be implemented using the `kernlab` package (Karatzoglou et al., 2004) in R.

S.1.3 Simulation Result

The comparison result of ITRs estimated from the proposed method and alternative models are shown in Table S1 and Figure S1.

From Table S1, we can observe that the ITRs estimated from the proposed method consistently have higher empirical values than those estimated from the version without group membership. Also, compared with the original assignment, the proposed method reduces the misclassification rate from 75% to around 20%, while the M-learning without group membership can not yield similar improvements.

From Figure S1, we see the ITRs estimated from the proposed method have higher empirical values than all four universal treatment rules. Therefore, we conclude that the implementation of group membership is essential to the propose approach and it can substantially improve the performance of the original M-learning proposed by Wu et al. (2020).

Table S1: Results of average means (standard deviations) of empirical value functions and misclassification rates (standard deviations) for 100 simulations.

Sample size	Model	Value	Misclassification
$N = 200$	M-learning, using group membership	**2.18**(0.13)	**0.14**(0.04)
	M-learning, without group membership	1.55(0.19)	0.76(0.03)
	Original assignment	1.38(-)	0.76(-)
$N = 400$	M-learning, using group membership	**2.22**(0.11)	**0.26**(0.04)
	M-learning, without group membership	1.81(0.14)	0.71(0.02)
	Original assignment	1.26(-)	0.78(-)
$N = 800$	M-learning, using group membership	**2.19**(0.10)	**0.20**(0.04)
	M-learning, without group membership	2.03(0.11)	0.71(0.01)
	Original assignment	1.26(-)	0.74(-)

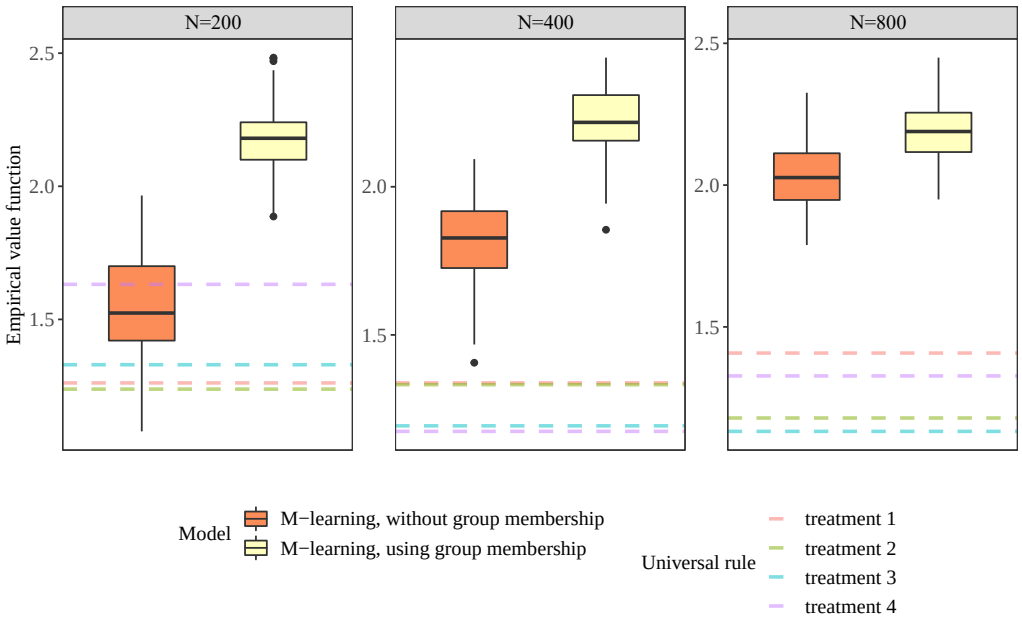

Figure S1: The empirical value function of ITRs using 5-fold cross-validation with 100 repeats (a higher value is more desirable).

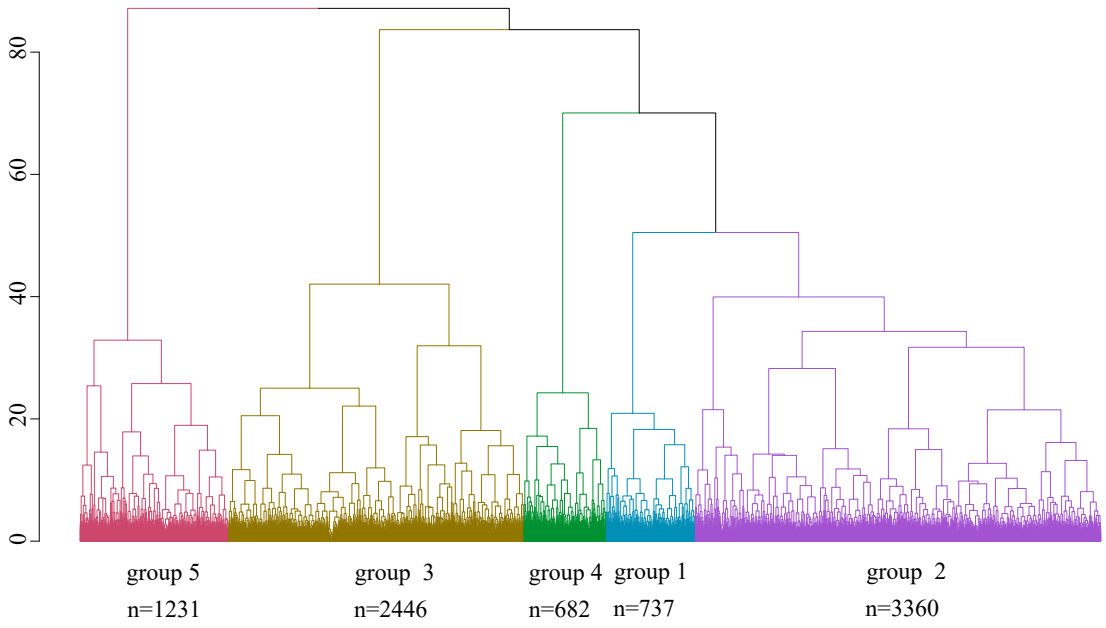

Figure S2: Dendrogram of Mahalanobis distances for 8,456 patients in electronic health records of the Ohio State University Wexner Medical Center.

S.2 Cluster Analysis in EHRs Analysis

S.2.1 Hierarchical Clustering

As described in the last second paragraph of Section 3.1 of the main document, we computed the similarity between each pair of patients using the Mahalanobis distance. which was defined in Section 2.1 of the main document. To compute the estimated latent processes $\widehat{\boldsymbol{\epsilon}}_i(t)$, we substituted health marker values $\boldsymbol{Y}_i(t)$ with the nearest neighbor observation of time t for patient i. Using the between-patient similarity matrix, we performed a cluster analysis on the 8,456 patients.

To determine the optimal number of patient groups, we calculated the point-biserial correlation (PBC) coefficient (Hennig and Liao, 2010; Milligan and Cooper, 1985) using R package `WeightedCluster` (Studer, 2013). PBC measures the capacity of the clustering to reproduce the distance matrix. We estimated the clustering quality for $2, 3, \ldots, 10$ groups, and, finally, we set the number of group to be 5, which maximized the absolute values of PBC. The dendrogram of the hierarchical clustering result is shown in Figure S2.

S.2.2 Consistency of Clustering Result

To examine the consistency of the clustering results, we adopted the idea of bootstrapping and estimated the probability of of two subjects being clustered into the same subgroup across

different partitions.

First of all, we resampled 8,456 patients with replacement from the 8,456 patients. The bootstrapped patients might have duplicates, so we only kept distinct patients. Next, we performed the hierarchical clustering on the Mahalanobis distance matrix of $\widehat{\boldsymbol{\epsilon}}_i(t)$ of the bootstrapped patients, and we still set the number of groups to 5. We denoted the resulted partition to d. Subsequently, we defined the relationship between a patient pair (i, j) as

$$R_d(i,j) = \begin{cases} 1 & \text{if patients } i \text{ and } j \text{ in the same group} \\ 0 & \text{if patients } i \text{ and } j \text{ belong to different groups} \end{cases}, \text{ for partition } d.$$

Then, we estimated the probability of of two subjects being clustered into the same subgroup across the original partition d_0 and bootstrapped partitions d by

$$P_d = \frac{\sum_{(i,j)\in d} \mathbb{I}\left(R_d(i,j) = R_{d_0}(i,j)\right)}{\text{Total number of } (i,j) \in d}.$$

Lastly, we reproduced 100 bootstrapped partitions and used the average P_d as the finalized estimator. For our EHR data, the average number of the bootstrapped patients is 5346.810 with a standard deviation of 26.701, and $\hat{P}_d$ is 0.716 with a standard deviation of 0.022. This result implies our clustering result is relatively robust.

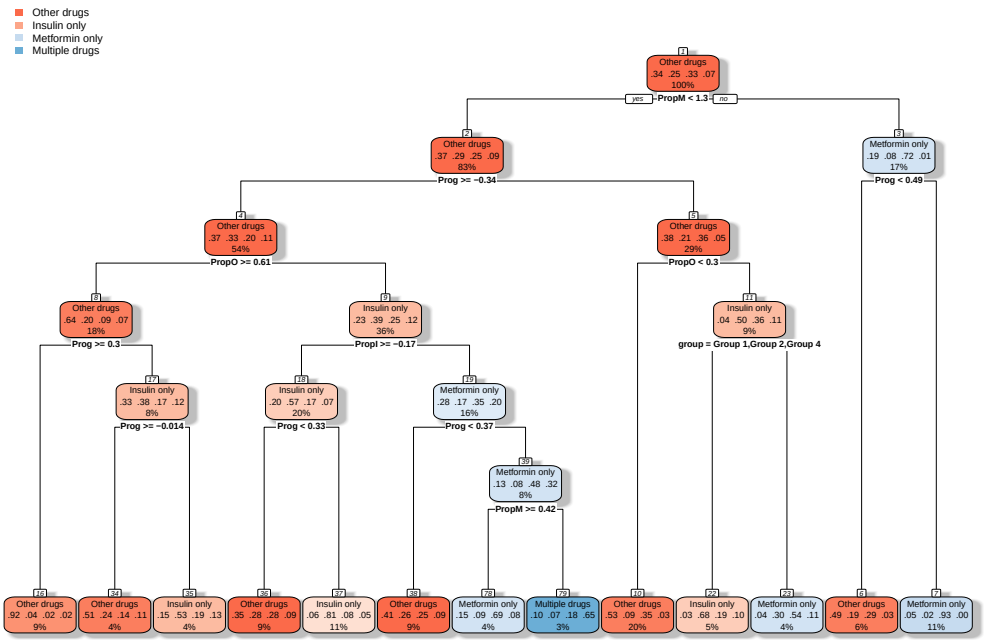

Figure S3: A decision tree model for the optimal ITRs. Prog: prognostic score. Prog: prognostic score. PropI: propensity score for insulin monotherapy. PropO: propensity score for other T2D drugs. PropM: propensity score for metformin monotherapy. group: group membership of patients.

S.3 ITRs in EHRs Analysis

S.3.1 Interpretable ITRs

To provide a better interpretation of the complicated non-linear ITRs to physicians, we used a simpler decision tree model to approximate the optimal ITRs in Section 4.2 of the main document.

As shown in Figure S3, the decision tree model only uses the three propensity scores, prognostic score, and group membership in its final treatment rule to recommend treatments. The treatment rule of the decision tree model has an accuracy of 63.0% to the optimal ITR of the proposed M-learning, but it is much easier to interpret to patients. There are other decision trees that have higher accuracy but deeper structures, so, in practice, physicians can select the most appropriate model based on their trade off between explainability and accuracy.

Lastly, we investigated the feature importance of the features in the decision tree model using R package `rpart` (Therneau and Atkinson, 2019). As shown in Figure S4, the most informative features are the prognostic score, three propensity scores, recent 1-year average HbA1c, and group membership. This result corresponds to the finding in Section 4.3 of the main document.

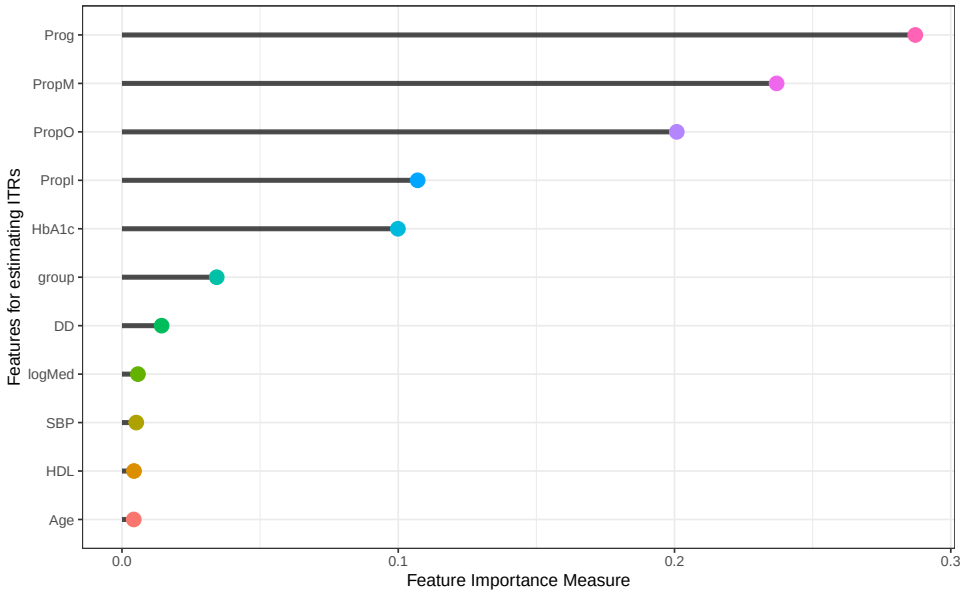

Figure S4: Feature importance of the decision tree model (the higher the value the more important the feature). Prog: prognostic score. PropI: propensity score for insulin monotherapy. PropO: propensity score for other T2D drugs. PropM: propensity score for metformin monotherapy. group: group membership of patients.

S.3.2 Agreement on Recommended and Observed Treatments

Table S2 displays the contingency table of observed treatments and the estimated ITRs recommendations. For metformin monotherapy, observed treatments and ITRs are matched by about 50% to 60% times. The proportion of other T2D drugs ranges from 40% to 60% across patient groups. Nevertheless, the observed insulin monotherapy merely has about a 30% to 40% match rate with ITRs. Particularly, in group 3, 4 and 5 of which patients have the highest HbA1c measurements, ITRs tend to assign metformin and other T2D drugs to more than 65% of patients who originally received insulin.

We also investigated the agreement of the observed prescriptions and estimated ITRs using the Cohen's kappa coefficient κ (Cohen, 1960). As shown in Table S3, all of the κ coefficients for the 4×4 contingency tables of group 1 to 5 (rows "overall") are between 0.179 and 0.247. McHugh (2012) suggested any κ value below 0.4 indicates at least moderate disagreement between the two categorical variables. Therefore, this result reveals the moderate disagreement between the observed prescriptions and estimated ITRs in all the identified patient subgroups. Moreover, we decomposed the "overall" disagreement to individual treatment class level by comparing each of the four treatment classes versus the rest. The κ values for all comparisons are less than 0.4, suggesting the consistent disagreement of all treatment classes. Particularly, for the assignments of insulin monotherapy in group 1 and metformin monotherapy in group 4, the κ coefficients are not significantly different from 0 (p-values are 0.643 and 0.050, respectively), so we could not reject the null hypothesis that the agreement is the same as chance agreement in these two cases.

Table S2: Contingency tables of four treatment classes by observed prescriptions (rows) and estimated ITRs (columns).

Group		Other drugs	Insulin only	Metformin only	Multiple drugs	Total in prescriptions
Group 1	Other drugs	42	41	5	12	100
	Insulin only	43	55	38	9	145
	Metformin only	21	38	68	4	131
	Multiple drugs	11	28	15	15	69
	Total in ITRs	117	162	126	40	445
Group 2	Other drugs	242	200	55	40	557
	Insulin only	160	199	124	27	510
	Metformin only	319	17	342	7	685
	Multiple drugs	44	44	109	40	237
	Total in ITRs	765	480	630	114	1989
Group 3	Other drugs	168	82	116	19	385
	Insulin only	183	152	95	13	443
	Metformin only	69	127	237	14	447
	Multiple drugs	71	46	40	46	203
	Total in ITRs	491	407	488	92	1478
Group 4	Other drugs	52	20	10	6	88
	Insulin only	13	50	87	2	152
	Metformin only	20	2	28	3	53
	Multiple drugs	23	5	25	27	80
	Total in ITRs	108	77	150	38	373
Group 5	Other drugs	93	30	38	34	195
	Insulin only	115	94	88	23	320
	Metformin only	37	36	156	25	254
	Multiple drugs	17	11	25	18	71
	Total in ITRs	262	171	307	100	840

Table S3: Cohen's kappa coefficients for the agreement of observed prescriptions and estimated ITRs.

Group	Treatment	Value	SE	Z	P-value
Group 1	Overall	0.179	0.032	5.576	< 0.001
	Other drugs	0.191	0.051	3.757	< 0.001
	Insulin only	**0.022**	0.047	0.463	**0.643**
	Metformin only	0.338	0.048	6.973	< 0.001
	Multiple drugs	0.182	0.060	3.052	0.002
Group 2	Overall	0.180	0.015	11.877	< 0.001
	Other drugs	0.062	0.022	2.818	0.005
	Insulin only	0.204	0.024	8.477	< 0.001
	Metformin only	0.284	0.022	12.622	< 0.001
	Multiple drugs	0.163	0.031	5.318	< 0.001
Group 3	Overall	0.181	0.018	10.314	< 0.001
	Other drugs	0.129	0.026	4.886	< 0.001
	Insulin only	0.099	0.027	3.696	< 0.001
	Metformin only	0.280	0.026	10.610	< 0.001
	Multiple drugs	0.247	0.036	6.872	< 0.001
Group 4	Overall	0.247	0.031	7.851	< 0.001
	Other drugs	0.366	0.053	6.839	< 0.001
	Insulin only	0.224	0.047	4.744	< 0.001
	Metformin only	**0.083**	0.042	1.957	**0.050**
	Multiple drugs	0.371	0.060	6.163	< 0.001
Group 5	Overall	0.218	0.022	9.835	< 0.001
	Other drugs	0.192	0.036	5.396	< 0.001
	Insulin only	0.160	0.033	4.917	< 0.001
	Metformin only	0.337	0.034	9.970	< 0.001
	Multiple drugs	0.124	0.044	2.794	0.005

Note: In column "Treatment", for each group, "Overall" represents the 4×4 contingency table in Table S2. The other four labels represent the 2×2 contingency tables for each of the four treatment classes versus the rest, respectively; "Value" is the value of Cohen's kappa coefficient κ for the corresponding contingency table; "SE" is the asymptotic standard error of κ; "Z" is the test statistic for a z-test with the null hypothesis $\kappa = 0$; "P-value" is the p-value for the z-test.

S.4 Gauss-Hermite quadrature method for parameter estimation

When $g_k^{-1}(z)$ takes a general form, we can compute the expectations $\mathbb{E}\left[Y_{ik}(t)|\boldsymbol{X}_i\right]$ and $\mathbb{E}\left[Y_{ik}(t)Y_{il}(t)|\boldsymbol{X}_i\right]$ using the Gauss-Hermite quadrature method (Abramowitz and Stegun, 1965). Suppose Q is the number of mass points, p_q are the mass points, and w_q are weights. Then

$$\begin{aligned}
\mathbb{E}\left[Y_{ik}(t)|\boldsymbol{X}_i\right] &\approx \sum_{q=1}^{Q} \frac{w_q}{\sqrt{\pi}} g_k^{-1}(\boldsymbol{X}_i^T\boldsymbol{\beta}_k(t) + \sqrt{2c_k}p_q), \\
\mathbb{E}\left[Y_{ik}(t)Y_{il}(t)|\boldsymbol{X}_i\right] &\approx \sum_{q_1=1}^{Q}\sum_{q_2=1}^{Q} \frac{w_{q_1}}{\sqrt{\pi}}\frac{w_{q_2}}{\sqrt{\pi}} \\
&\quad \times g_k^{-1}\left(\boldsymbol{X}_i^T\widehat{\boldsymbol{\beta}}_k(t) + \sqrt{2c_k}p_{q_1}[\boldsymbol{R}_{kl}(t)]_{1,1} + \sqrt{2c_k}p_{q_2}[\boldsymbol{R}_{kl}(t)]_{2,1}\right) \\
&\quad \times g_l^{-1}\left(\boldsymbol{X}_i^T\widehat{\boldsymbol{\beta}}_l(t) + \sqrt{2c_l}p_{q_1}[\boldsymbol{R}_{kl}(t)]_{1,2} + \sqrt{2c_l}p_{q_2}[\boldsymbol{R}_{kl}(t)]_{2,2}\right),
\end{aligned}$$

where $\boldsymbol{R}_{kl}(t)$ is chosen as the 2×2 square-root matrix of $\boldsymbol{\Sigma}_{kl}(t)$, and $[\boldsymbol{R}_{kl}(t)]_{i,j}$ denotes the entry in the ith row and jth column of $\boldsymbol{R}_{kl}(t)$.

On the other hand, we can compute $\mathbb{E}\left[\boldsymbol{\epsilon}_i(t)\middle|\boldsymbol{Y}_i(t), \widehat{\boldsymbol{\beta}}_k(t), \widehat{\sigma}_{kl}(t)\right]$ as follows,

$$\begin{aligned}
&\mathbb{E}\left[\boldsymbol{\epsilon}_i(t)\middle|\boldsymbol{Y}_i(t), \widehat{\boldsymbol{\beta}}_k(t), \widehat{\sigma}_{kl}(t)\right] \\
=\ & \frac{\int \mathbb{P}\left(\boldsymbol{Y}_i(t)|\boldsymbol{\epsilon}_i(t)\right)\mathbb{P}\left(\boldsymbol{\epsilon}_i(t)\right)\boldsymbol{\epsilon}_i(t)d\boldsymbol{\epsilon}_i(t)}{\int \mathbb{P}\left(\boldsymbol{Y}_i(t)|\boldsymbol{\epsilon}_i(t)\right)\mathbb{P}\left(\boldsymbol{\epsilon}_i(t)\right)d\boldsymbol{\epsilon}_i(t)} \\
=\ & \frac{\int_D \prod_{k=1}^{p}\left[f_{ik}\left(y_{ik}(t); \boldsymbol{X}_i^T\widehat{\boldsymbol{\beta}}_k(t) + \epsilon_{ik}(t), \hat{\phi}_{ik}\right)\epsilon_{ik}(t)\right] f\left(\boldsymbol{\epsilon}_i(t); \widehat{\boldsymbol{\Omega}}(t)\right)d\boldsymbol{\epsilon}_i(t)}{\int_D \prod_{k=1}^{p} f_{ik}\left(y_{ik}(t); \boldsymbol{X}_i^T\widehat{\boldsymbol{\beta}}_k(t) + \epsilon_{ik}(t), \hat{\phi}_{ik}\right) f\left(\boldsymbol{\epsilon}_i(t); \widehat{\boldsymbol{\Omega}}(t)\right)d\boldsymbol{\epsilon}_i(t)} \\
\approx\ & \frac{\sum_{q_\cdot=1}^{Q}\prod_{k=1}^{p}\left[f_{ik}\left(y_{ik}(t); \boldsymbol{X}_i^T\widehat{\boldsymbol{\beta}}_k(t) + h_k\left(p_q, \widehat{\boldsymbol{\Omega}}(t)\right), \hat{\phi}_{ik}\right)h_k\left(p_q, \widehat{\boldsymbol{\Omega}}(t)\right)w_{q_k}\right]}{\sum_{q_\cdot=1}^{Q}\prod_{k=1}^{p}\left[f_{ik}\left(y_{ik}(t); \boldsymbol{X}_i^T\widehat{\boldsymbol{\beta}}_k(t) + h_k\left(p_q, \widehat{\boldsymbol{\Omega}}(t)\right), \hat{\phi}_{ik}\right)w_{q_k}\right]},
\end{aligned}$$

where $\sum_{q_\cdot=1}^{Q} \equiv \sum_{q_1=1}^{Q}\cdots\sum_{q_p=1}^{Q}$. Furthermore, $f_{ik}(\cdot)$ is the density function of $Y_{ik}(t)$, and $f\left(\boldsymbol{\epsilon}_i(t); \widehat{\boldsymbol{\Omega}}(t)\right)$ is the density function of a multivariate normal distribution with mean $\mathbf{0}$ and covariance matrix $\widehat{\boldsymbol{\Omega}}(t)$. Lastly, $h_k\left(p_q, \widehat{\boldsymbol{\Omega}}(t)\right) = \sqrt{\frac{2c_k}{\pi}}\sum_{l=1}^{p} p_{q_l}\left[\widetilde{\boldsymbol{R}}(t)\right]_{k,l}$ with $\widetilde{\boldsymbol{R}}(t)$ being the square-root matrix of $\widehat{\boldsymbol{\Omega}}(t)$, and $[\widetilde{\boldsymbol{R}}(t)]_{k,l}$ is the entry in the kth row and lth column of $\widetilde{\boldsymbol{R}}(t)$.

References

Abramowitz, M. and Stegun, I. (1965). *Handbook of Mathematical Functions: With Formulas, Graphs, and Mathematical Tables*. Applied mathematics series. Dover Publications, New York, NY, USA.

Cohen, J. (1960). A coefficient of agreement for nominal scales. *Educational and Psychological Measurement* **20,** 37–46.

Hennig, C. and Liao, T. F. (2010). Comparing latent class and dissimilarity based clustering for mixed type variables with application to social stratification. Technical report, Research Report No. 308, Department of Statistical Science, University College London.

Karatzoglou, A., Smola, A., Hornik, K., and Zeileis, A. (2004). kernlab – an s4 package for kernel methods in R. *Journal of Statistical Software* **11,** 1–20.

Kuhn, M. (2008). Building predictive models in R using the caret package. *Journal of Statistical Software, Articles* **28,** 1–26.

McHugh, M. L. (2012). Interrater reliability: the kappa statistic. *Biochemia Medica* **22,** 276–282.

Milligan, G. and Cooper, M. (1985). An examination of procedures for determining the number of clusters in a data set. *Psychometrika* **50,** 159–179.

Studer, M. (2013). WeightedCluster library manual: a practical guide to creating typologies of trajectories in the social sciences with R. Technical report, LIVES Working Papers 24.

Therneau, T. and Atkinson, B. (2019). *rpart: recursive partitioning and regression trees*. R package version 4.1-15.

Wu, P., Zeng, D., and Wang, Y. (2020). Matched learning for optimizing individualized treatment strategies using electronic health records. *J. Amer. Statist. Assoc.* **115,** 380–392.